note that the interatomic distances between the Re atoms centering these face-joined octahedra [Re(1)–Re(1) at 3·12 and Re(2)–Re(2) at 3·61 Å] are notably different. They are also notably longer than the interatomic distances between the Re atoms centering the face-joined octahedron columns [2·66 and 2·75 Å].

$Sc_5Re_8Si_{12}$ belongs to the category of structures built up with columns of square antiprisms and octahedra which has been discussed recently by Chabot & Parthé (1985). It has been shown above that the $Sc_5Re_8Si_{12}$ structure can be described as an arrangement of $Hf_2Ru_3Si_4$-type slabs with interspersed monoatomic layers. Similarly, $ZrMnSi_2$ (Venturini, Steinmetz & Roques, 1982) can be described as an arrangement of deformed $Sc_3Re_2Si_4$-type slabs [parallel to $(1\bar{1}0)$ in $ZrMnSi_2$] with another kind of interspersed monoatomic layer.

We acknowledge the help of Mrs B. Künzler with the preparation of the drawing and Dr J. Steinmetz and Mr J. M. Claude (Laboratoire de Microanalyse, Université de Nancy I, France) for the electron microprobe analysis. This study was supported by the Swiss National Science Foundation under contract No. 2.035-0.86.

References

Becker, P. J. & Coppens, R. (1974). *Acta Cryst.* A**30**, 129–147.
Bernardinelli, G. & Flack, H. D. (1985). *Acta Cryst.* A**41**, 500–511.
Brown, I. D. (1985). *Acta Cryst.* A**41**, 399.
Chabot, B. & Parthé, E. (1985). *Acta Cryst.* B**41**, 213–219.
Chabot, B., Parthé, E. & Braun, H. F. (1985). *Acta Cryst.* C**41**, 1148–1152.
Flack, H. D. (1983). *Acta Cryst.* A**39**, 876–881.
Flack, H. D. & Schwarzenbach, D. (1987). *Acta Cryst.* A**43**. In preparation.
International Tables for X-ray Crystallography (1974). Vol. IV. Birmingham: Kynoch Press. (Present distributor D. Reidel, Dordrecht, The Netherlands.)
Pecharskii, V. K. (1979). Autoreferat Dis. Kand. Khim. (Abstract of thesis in Russian). Lvov: Nauk.
Pecharskii, V. K., Bodak, O. I. & Gladyshevskii, E. I. (1978). *Dopov. Akad. Nauk Ukr. RSR Ser. A*, pp. 755–759.
Pecharskii, V. K., Bodak, O. I. & Gladyshevskii, E. I. (1979). *Sov. Phys. Crystallogr.* **24**, 433–438.
Rogl, P. (1984). In *Handbook on the Physics and Chemistry of Rare Earths*, Vol. 7, edited by K. A. Gschneidner & L. Eyring, ch. 51. Amsterdam: North-Holland.
Stewart, J. M., Machin, P. A., Dickinson, C. W., Ammon, H. L., Heck, H. & Flack, H. (1976). The *XRAY76* system. Tech. Rep. TR-446. Computer Science Center, Univ. of Maryland, College Park, Maryland, USA.
Venturini, G., Steinmetz, J. & Roques, B. (1982). *J. Less-Common Met.* **87**, 21–30.

Acta Cryst. (1987). C**43**, 1668–1674

Orthorhombic Perovskite $CaTiO_3$ and $CdTiO_3$: Structure and Space Group

By Satoshi Sasaki,* Charles T. Prewitt† and Jay D. Bass‡

Department of Earth and Space Sciences, State University of New York, Stony Brook, NY 11794, *USA*

and Walter A. Schulze

Materials Research Laboratory, The Pennsylvania State University, University Park, PA 16802, *USA*

(*Received* 6 *August* 1985; *accepted* 13 *May* 1987)

Abstract. Structural aspects and physical properties strongly indicate that the $CdTiO_3$ perovskite has a centrosymmetric structure with space group *Pbnm*. Single-crystal X-ray studies have revealed that both $CaTiO_3$ and $CdTiO_3$ can be described well as $GdFeO_3$-type perovskites in terms of the size ratio of two kinds of cation occupying *A* and *B* sites. Distortions and tiltings of polyhedra are systematically related to the *observed tolerance factor*. The crystal data for $CaTiO_3$ are: $M_r = 135{\cdot}98$, *Pbnm*, $a = 5{\cdot}3796\,(1)$, $b = 5{\cdot}4423\,(3)$, $c = 7{\cdot}6401\,(5)$ Å, $V = 223{\cdot}68\,(1)$ Å^3, $Z = 4$, $D_x = 4{\cdot}04$ g cm^{-3}, Mo $K\alpha$, $\lambda = 0{\cdot}7107$ Å, $\mu = 58{\cdot}0$ cm^{-1}, $F(000) = 264$, $T = 293$ K, $R = 0{\cdot}023$, 703 unique reflections used for refinements, crystal synthesized at 1470 K and 2·5 GPa. The crystal data for $CdTiO_3$ are: $M_r = 208{\cdot}30$, *Pbnm*, $a = 5{\cdot}3053\,(1)$, $b = 5{\cdot}4215\,(3)$, $c = 7{\cdot}6176\,(3)$ Å, $V = 219{\cdot}10\,(1)$ Å^3, $Z = 4$, $D_x = 6{\cdot}31$ g cm^{-3}, Mo $K\alpha$, $\lambda = 0{\cdot}7107$ Å, $\mu = 130{\cdot}6$ cm^{-1}, $F(000) = 376$, $T = 293$ K, $R = 0{\cdot}019$, 829 unique reflections, crystal synthesized at 1470 K and 1·5 GPa.

---

* Present address: The Photon Factory, National Laboratory for High-Energy Physics, Oho-machi, Ibaraki 305, Japan.

† Present address: Geophysical Laboratory, 2801 Upton Street, NW, Washington, DC 20008, USA

‡ Present address: Department of Geology, University of Illinois, Urbana, IL 61801, USA.

0108-2701/87/091668-07$01.50

Introduction. Historically, both $CaTiO_3$ and $CdTiO_3$ are known to crystallize with orthorhombic distortions of the perovskite structure, based on the observation of powder X-ray films (Náray-Szabó, 1943; Megaw, 1946). By using the single-crystal film method, Kay & Bailey (1957) and Kay & Miles (1957) assigned probable space groups for $CaTiO_3$ and $CdTiO_3$ to be *Pbnm* and $Pbn2_1$, respectively. The main difference between these two arrangements, if detectable, would be in the deviation of the divalent cations from the mirror plane of *Pbnm*.

The mineral perovskite ($CaTiO_3$) is one of the few minerals having the distorted perovskite structure, although it has been suggested that the Earth's lower mantle may be composed largely of $MgSiO_3$ perovskite (for example, Yagi, Mao & Bell, 1978). Because structural parameters of $CaTiO_3$ derived from the X-ray film study of Kay & Bailey (1957) deviate markedly from the systematic plots of other $GdFeO_3$-type perovskites (Sasaki, Prewitt & Liebermann, 1983), we refined its crystal structure. A powder neutron study has been reported for this crystal (Koopmans, van de Velde & Gellings, 1983). For $CdTiO_3$, the $Pbn2_1$ structure* reported by Kay & Miles (1957) is characterized by a large displacement of Ti atoms along the *b* axis and a lack of equality between the atomic positions of O(2) and O(2)(2). In their measurement of electrical properties, Sholokhovich, Kramarov, Proskuryakov & Éknadiosyants (1969) could not resolve whether $CdTiO_3$ single crystals were ferroelectric. The present work is the consequence of two technical advances over previous studies: (1) use of a four-circle diffractometer instead of film techniques; (2) synthesis of untwinned single crystals of $CaTiO_3$ and $CdTiO_3$; and (3) more sensitive tests for the absence of a center of symmetry in the crystal. The purpose of this paper is to present new crystallographic data and refinement of the structure of $CaTiO_3$ and to clarify the space group for $CdTiO_3$.

Experimental. The crystals of $CaTiO_3$ were grown from equimolar mixtures of CaO and TiO_2 at 1470 K and 2·5 GPa for 40 min, using a girdle-anvil solid-media apparatus equipped with an internal graphite heater (Liebermann, Ringwood, Mayson & Major, 1975). The starting materials were loaded into a Pt capsule with the open ends crimped tight, welded shut, and cold-pressed with the aid of a pellet press. The crystals of $CdTiO_3$ were synthesized in a piston-cylinder apparatus (Boyd & England, 1960) from equimolar mixtures of CdO and TiO_2 at 1470 K and 1·5 GPa for 60 min. A quantity of H_2O (10–15%) was present in each charge to promote crystal growth.

Some of the crystals of $CaTiO_3$ and $CdTiO_3$ looked untwinned under the polarizing microscope but, using X-ray precession photography, almost all crystals were found to be twinned. Finally, an untwinned crystal for each compound was found; the crystals are transparent and approximately parallelepiped in shape with dimensions $70 \times 60 \times 50$ µm for $CaTiO_3$ and $70 \times 60 \times 60$ µm for $CdTiO_3$. The unit cell was determined for each crystal from a least-squares fit to positions of 20 reflections in the range $43 \leq 2\theta \leq 68°$. Each reflection was centered at eight different equivalent positions of the Picker four-circle diffractometer (graphite-monochromatized Mo $K\alpha_1$ radiation; $\lambda = 0{\cdot}70926$ Å). The precession photographs and the intensity data from the four-circle diffractometer verified that the Laue symmetry of each crystal is *mmm* and the systematic absences are: no conditions on *hkl*; $k = 2n$ on $0kl$; $h + l = 2n$ on $h0l$; no conditions on $hk0$. The possible space group for each crystal is either D^{16}_{2h}–*Pbnm* or C^{9}_{2v}–$Pbn2_1$.

Integrated intensity data up to $2\theta = 90°$ were collected using the ω–2θ scan mode of the four-circle diffractometer with a scan width of $2{\cdot}0 + 0{\cdot}7\tan\theta$ (° in 2θ). The scan speed and time for each reflection were varied so as to obtain $\sigma_I/I = 0{\cdot}01$ or to measure up to 300 s. The range of *hkl* values measured is: $0 \leq h \leq 10$, $0 \leq k \leq 10$, and $0 \leq l \leq 15$. Of 973 independent reflections measured for $CaTiO_3$, there were 703 for which $I_{\rm obs} \geq 2\sigma_I$ and could be used for refinement. Likewise, 829 of the 956 independent reflections collected for $CdTiO_3$ were used. One standard reflection, 532, was measured for each crystal; the variation in $I_{\rm obs}$ was $\pm 1{\cdot}9\%$ for $CaTiO_3$ and $\pm 2{\cdot}6\%$ for $CdTiO_3$. Each set of intensities was corrected for Lorentz and polarization factors. An integration method for the absorption correction was applied to each crystal, using the program *ACACA* (Wuensch & Prewitt, 1965). The transmission factors varied from 0·706 to 0·765 for $CaTiO_3$ and from 0·401 to 0·525 for $CdTiO_3$.

All parameters (scale factor, secondary-extinction parameter, atom coordinates and anisotropic temperature factors) were refined simultaneously using the full-matrix least-squares program *RADY* (Sasaki *et al.*, 1983; originally *ORFLS* by Busing, Martin & Levy, 1963). The residuals of the function $\sum w_i(|F_o| - |F_c|)^2_i$ were minimized with $w_i = 1/\sigma^2_F$, where

$$\sigma_F = S\{C_t/T^2_m + \tfrac{1}{2}(B_g/B_t) + I_{\rm obs}\varepsilon\}^{1/2},$$

s is the scan width, C_t is the total counts under a peak, T_m is the time to record a peak, B_g is background count, B_t is background time, $I_{\rm obs}$ is integrated intensity and $\varepsilon = 0{\cdot}9 \times 10^{-7}$. The structural refinements for $CaTiO_3$ were based on space group *Pbnm*. The final *R* and *wR* values are 0·023 and 0·029, respectively, and the goodness of fit is 1·10. For the $CdTiO_3$ crystal, the refinements were made by using models for both *Pbnm* and $Pbn2_1$. It should be noted that the difference in

---

* Although Kay & Miles (1957) reported space group $Pc2_1n$, $Pbn2_1$ is used here on the basis of the standard definition for perovskites.

Table 1. *Atomic coordinates and equivalent isotropic temperature factors of* $CaTiO_3$ *and* $CdTiO_3$ *perovskites*

The results of $CdTiO_3$ are based on both *Pbnm* and $Pbn2_1$ models and are compared with the previous results of Kay & Miles (1957).

KM: Kay & Miles (1957); KVG: Koopmans *et al.* (1983).

	$CaTiO_3$ *Pbnm*		$CdTiO_3$ *Pbnm*	$CdTiO_3$ $Pbn2_1$ (model)	
	This study	KVG	This study	This study	KM
Ca sites					
x	−0·00676 (7)	−0·0083 (7)	−0·00847 (3)	−0·00843 (3)	−0·006
y	0·03602 (6)	0·0360 (5)	0·03873 (3)	0·03871 (3)	−0·016
z	$\frac{1}{4}$	$\frac{1}{4}$	$\frac{1}{4}$	$\frac{1}{4}$*	$\frac{1}{4}$
B_{eq}	0·612 (5)	1·01 (7)	0·608 (4)	0·613 (3)	
Ti sites					
x	0	0	0	−0·0011 (13)	0·095
y	$\frac{1}{2}$	$\frac{1}{2}$	$\frac{1}{2}$	0·5005†	0·435
z	0	0	0	−0·0009 (3)	0·0
B_{eq}	0·395 (4)	0·6 (1)	0·484 (6)	0·485 (6)	
O(1) sites					
x	0·0714 (3)	0·0726	0·0902 (3)	0·0898 (3)	0·03
y	0·4838 (2)	0·4827	0·4722 (3)	0·4721 (3)	0·45
z	$\frac{1}{4}$	$\frac{1}{4}$	$\frac{1}{4}$	0·244 (1)	0·25
B_{eq}	0·53 (2)	0·94 (6)	0·05 (2)	0·41 (3)	
O(2) sites					
x	0·7108 (2)	0·7099 (3)	0·7008 (2)	0·706 (1)	0·80
y	0·2888 (2)	0·2877 (3)	0·2969 (2)	0·304 (1)	0·19
z	0·0371 (1)	0·0369 (2)	0·0472 (2)	0·0482 (9)	0·007
B_{eq}	0·50 (1)	0·94 (6)	0·55 (2)	0·53 (6)	
O(2) (2) sites					
x				0·696 (1)	0·80
y				0·290 (1)	0·19
z				0·4538 (9)	0·47
B_{eq}				0·49 (6)	

* The z coordinate of Cd atoms is defined as $\frac{1}{4}$.

† The y coordinate of Ti atoms for this model was fixed because of the oscillation by ±0·003 around $\frac{1}{2}$ (see Table 3).

atomic coordinates between centrosymmetric and non-centrosymmetric $CdTiO_3$ models is very small and the refinements converged with similar R factors: $R = 0{\cdot}019$ and $wR = 0{\cdot}030$ (goodness of fit = 1·25) for the *Pbnm* model; $R = 0{\cdot}018$ and $wR = 0{\cdot}027$ (goodness of fit = 1·14) for the $Pbn2_1$ model. Ratios of maximum least-squares shift to e.s.d. in final refinement cycles are $4{\cdot}8 \times 10^{-4}$ for $CaTiO_3$ and $3{\cdot}5 \times 10^{-3}$ and $1{\cdot}6 \times 10^{-3}$ for $CdTiO_3$ (*Pbnm* and $Pbn2_1$ models), respectively. Atomic scattering factors and anomalous-dispersion coefficients were taken from *International Tables for X-ray Crystallography* (1974) and Tokonami (1965). Secondary-extinction parameters, g (Becker & Coppens, 1974) are $1{\cdot}6 \times 10^{-3}$ and $3{\cdot}9 \times 10^{-3}$ for $CaTiO_3$ and $CdTiO_3$, respectively. The results of structural refinements for $CaTiO_3$ and $CdTiO_3$ are given in Table 1 which includes atomic coordinates and temperature factors.* Difference Fourier syntheses calculated after the final refinements showed minimum and maximum values of −1·3, 1·0 e Å^{-3} for $CaTiO_3$ and −1·1, 1·7 e Å^{-3} for $CdTiO_3$.

Discussion.

Space-group determination

(1) *Statistical probability of intensity distribution.* The space groups of $CaTiO_3$ and $CdTiO_3$ are either *Pbnm* (centrosymmetric) or $Pbn2_1$ (non-centrosymmetric) on the basis of the information above. Some information about the probable presence or absence of a center of symmetry in a crystal should be contained in the 'probability distribution' of the observed intensity. For example, the ratio $r = \langle |F| \rangle^2/\langle I \rangle$ may indicate the presence (= 0·637) or absence (= 0·785) of a center of symmetry (Wilson, 1949). The r values calculated for $CaTiO_3$ and $CdTiO_3$ are 0·531 and 0·590, respectively. It is also possible to determine the probability distribution of the intensities. with the zero-moment test reported by Howells, Phillips & Rogers (1950). There is a considerable difference in $N(z)$ between the centric and acentric distributions, where $N(z)$ is the fraction of reflections with $I < z\langle I \rangle$ as a function of $z = I/\langle I \rangle$. As seen in Fig. 1, $N(z)$ for the centrosymmetric structure is greater than for the non-centrosymmetric structure for all values. The distortion plots for $CaTiO_3$ and $CdTiO_3$ in Fig. 1 are similar and resemble the $N(z)$ curve for the centrosymmetric structure both in value of $N(z)$ and in curvature.

Another effect can be detected in particular projections of the space groups, *Pbnm* and $Pbn2_1$. The presence of the mirror plane should be expected to increase the average intensity of the $hk0$ reflections, because each atom in the unit cell appears on top of its mirror-related image. Therefore, it is interesting to estimate the ratio $\sigma_{hk0} = \langle I \rangle_{hk0}/\langle I \rangle_{hkl}$. The experi-

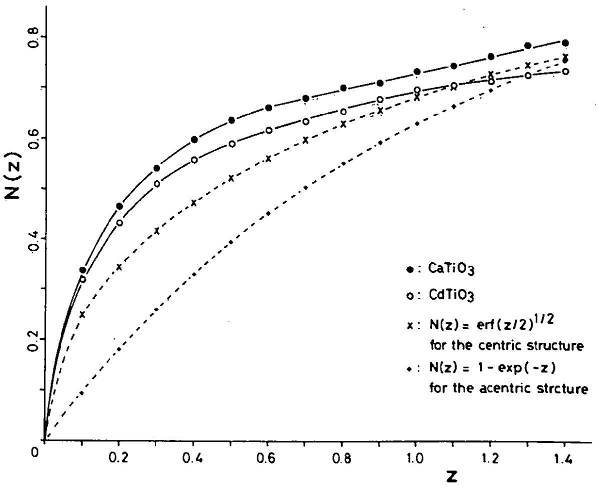

Fig. 1. Distribution plot of X-ray intensities for $CaTiO_3$ and $CdTiO_3$, compared with the ideal $N(z)$ values *versus* $z = I/\langle I \rangle$.

---

* Lists of structure factors and anisotropic temperature factors have been deposited with the British Library Document Supply Centre as Supplementary Publication No. SUP 43975 (20 pp.). Copies may be obtained through The Executive Secretary, International Union of Crystallography, 5 Abbey Square, Chester CH1 2HU, England.

mental ratios of σ_{hk0}, 2·4 ($CaTiO_3$) and 1·8 ($CdTiO_3$), are close to 2 which indicates the presence of the mirror elements ($\sigma_{hk0} = 1$ for absence). The σ values for *h*0*l* and 0*kl* reflections range between 2·4 and 2·5 for these specimens. It is clear that both experimental values are closer to that of space group *Pbnm*, although there is the possibility that the experimental distributions follow some kind of hypersymmetry.

(2) *Physical properties.* If crystals belong to space group $Pbn2_1$ and are piezoelectric, there should be a resonance between an oscillating electric field and the crystal. A piezoelectric oscillator with the frequency range of 1–14 MHz was used to detect this resonance (Giebe–Scheibe method) in $CdTiO_3$. The tests were negative, which suggests that the crystal is centrosymmetric or the resonance could not be detected. This result is consistent with the previous result reported by Sholokhovich *et al.* (1969).

The second-harmonic generation in crystalline powders gives useful information on the non-linear optical properties of crystals and makes possible the detection of small deviations from centrosymmetry (Kurtz & Perry, 1968). We have used in this study the apparatus of Bish, Horsey & Newnham (1979) with the additional improvements of higher-bandwidth electronics and a cooled photomultiplier-tube housing for noise reduction.

The $CdTiO_3$ sample had a signal lower than could be measured on the equipment. The signal appeared to be at least three orders of magnitude weaker than quartz or five orders weaker than $BaTiO_3$ at room temperature. This test cannot determine a zero signal and ultimately other factors will produce extremely weak signals. Although only a positive test for non-centrosymmetry has significance, this test suggests that there is no reason to infer a non-centrosymmetric structure.

(3) *Structural approach.* The previous X-ray study proposed a non-centrosymmetric $Pbn2_1$ structure for $CdTiO_3$ (Kay & Miles, 1957). Most of the arguments were based on the differences between $|F_o|$ and $|F_c|$ for the 0*kl* reflections (k = odd; l = odd); Kay & Miles concluded that the differences could be explained by the systematic shift in the atomic coordinates of Ti and O atoms from the *Pbnm* structure. However, the observed structure factors for 0*kl* reflections obtained in our study (*Pbnm* model) do not have such a discrepancy (see Table 2). The intensity variation in Kay & Miles's (1957) data could be experimental errors resulting from the film techniques. Since Kay & Miles (1957) also indicated a large displacement of the Ti atoms along the y axis, residual factors of the least-squares calculation were computed by changing the y coordinate of Ti atoms (Table 3). The residual factors have a minimum near $y = 0·5$ on a parabola. Therefore, it is more suitable to assign the space group of $CdTiO_3$ as *Pbnm*, rather than the polar group $Pbn2_1$ suggested by Kay & Miles (1957).

Table 2. *The structure-factor tables for* 0*kl*, *h*0*l and* *hk*0 *reflections of* $CdTiO_3$ *based on the least-squares calculation of a Pbnm model*

The list includes only reflections described in Kay & Miles (1957); the other reflections are given in deposited tables.

			This study			Kay & Miles (1957)	
h	*k*	*l*	$\lvert F_{obs}\rvert$	$\lvert F_{calc}\rvert$	σ_F	$\lvert F_{obs}\rvert$	$\lvert F_{calc}\rvert$
0*kl*							
0	2	1	53·04	53·45	0·85	21·1	17·8
0	2	3	69·28	70·05	1·15	24·0	23·0
0	2	5	32·32	31·82	0·56	10·0	11·8
0	2	7	44·13	43·41	0·77	13·0	14·8
0	2	9	25·64	25·25	0·51	7·6	9·2
0	4	1	82·68	85·72	1·40	30·0	25·7
0	4	3	57·76	58·31	0·98	19·9	16·6
0	4	5	77·97	77·88	1·35	24·9	24·4
0	4	7	42·75	42·35	0·77	12·5	12·5
0	4	9	48·25	47·69	0·90	12·9	14·4
0	4	11	35·60	35·54	0·73	10·0	13·2
0	6	1	61·74	62·95	1·08	19·9	19·6
0	6	3	71·95	73·21	1·27	23·0	22·6
0	6	5	45·16	45·89	0·83	13·6	17·1
0	6	7	57·34	58·32	1·07	16·6	19·1
0	6	9	38·47	38·04	0·77	10·5	15·8
0	8	1	44·81	46·26	0·86	13·5	19·0
0	8	3	36·36	37·27	0·72	11·1	18·3
0	8	5	44·66	45·09	0·88	12·1	18·6
*h*0*l*							
1	0	3	36·50	37·81	0·59	11·7	10·7
1	0	5	24·11	23·97	0·43	7·5	8·4
1	0	7	14·86	14·74	0·33	3·9	3·5
3	0	1	3·16	3·90	0·29	<3·0	1·2
3	0	3	16·65	16·99	0·32	5·6	7·0
3	0	5	7·01	7·48	0·29	<3·0	1·8
3	0	7	12·53	12·26	0·33	3·6	3·8
3	0	9	4·78	5·35	0·45	<3·0	2·0
5	0	1	19·80	20·31	0·39	6·2	4·9
5	0	3	18·08	18·63	0·38	5·5	4·7
5	0	5	17·22	17·06	0·39	6·1	4·9
5	0	7	14·63	14·54	0·39	4·5	4·2
5	0	9	12·00	11·88	0·41	3·0	3·8
7	0	1	27·69	27·93	0·55	8·3	6·7
7	0	3	20·72	20·44	0·46	5·7	4·1
7	0	5	28·01	28·41	0·58	8·5	7·9
7	0	7	16·28	16·10	0·45	4·9	4·5
7	0	9	19·89	20·33	0·52	5·5	5·2
9	0	1	21·32	21·67	0·52	5·4	5·1
9	0	3	28·34	28·61	0·63	7·8	8·1
9	0	5	14·02	14·73	0·48	3·0	3·2
9	0	7	25·21	24·64	0·61	6·6	7·1
*hk*0							
1	2	0	15·66	16·50	0·28	4·4	8·6
1	4	0	30·07	29·70	0·52	8·2	8·4
1	6	0	5·77	5·93	0·37	<3·0	2·5
2	1	0	24·00	25·06	0·40	7·6	7·8
2	3	0	13·41	12·75	0·28	3·5	3·5
3	2	0	22·99	23·16	0·41	6·4	4·6
3	4	0	8·93	8·53	0·28	<3·0	1·8
3	6	0	22·69	22·55	0·47	4·8	4·8
4	1	0	24·61	25·04	0·44	6·8	7·3
4	3	0	2·94	0·68	0·42	<3·0	0·1
5	2	0	12·23	12·24	0·31	3·3	1·6
5	4	0	17·59	17·29	0·40	4·0	2·5
5	6	0	15·85	15·24	0·42	3·6	2·9
6	1	0	5·60	5·61	0·41	<3·0	3·6
6	3	0	23·40	23·40	0·48	6·3	5·4
7	2	0	6·93	6·35	0·43	<3·0	0·7
7	4	0	20·32	19·89	0·48	4·8	4·5
7	6	0	8·72	8·68	0·48	<3·0	2·4

Interatomic distances and angles for both perovskites are given in Tables 4–6. The mean distances are $\langle \mathrm{Ca–O}\rangle^{\mathrm{xii}} = 2{\cdot}726$ Å ($\langle \mathrm{Ca–O}\rangle^{\mathrm{viii}} = 2{\cdot}519$ Å) and $\langle \mathrm{Ti–O}\rangle^{\mathrm{vi}} = 1{\cdot}955$ Å for $CaTiO_3$ and $\langle \mathrm{Cd–O}\rangle^{\mathrm{xii}} = 2{\cdot}718$ Å ($\langle \mathrm{Cd–O}\rangle^{\mathrm{viii}} = 2{\cdot}466$ Å) and $\langle \mathrm{Ti–O}\rangle^{\mathrm{vi}} = 1{\cdot}966$ Å for $CdTiO_3$. Both compounds satisfy the criterion for orthorhombic $GdFeO_3$-type perovskites. The degree of distortion and tilting of polyhedra is indicated schematically as a function of the *observed tolerance factor*

$$t_{\mathrm{obs}} = \langle A\text{–O}\rangle / 2^{1/2} \langle B\text{–O}\rangle,$$

where $\langle A\text{–O}\rangle$ and $\langle B\text{–O}\rangle$ are the mean interatomic distances with twelve and six coordination for *A* (Ca, Cd) and *B* (Ti) sites, respectively (Sasaki *et al.*, 1983). For the ideal cubic perovskites, $t_{\mathrm{obs}} = 1{\cdot}0$, so $CdTiO_3$ ($t_{\mathrm{obs}} = 0{\cdot}978$) is more distorted than $CaTiO_3$ ($t_{\mathrm{obs}} = 0{\cdot}986$). The t_{obs} values estimated in this study can be used to plot experimental curves of such crystal-

Table 3. *Residual factors and R values versus the y displacement of* Ti *sites for* $CdTiO_3$: $y = \frac{1}{2} + \Delta y$

All other variables based on the $Pbn2_1$ structure, scale and extinction factors are refined simultaneously with 829 reflections.

Δy	$\sum w(\lvert F_o\rvert - \lvert F_c\rvert)^2$	*R*	*wR*
−0·02	8283	0·0437	0·0766
−0·015	2725	0·0269	0·0439
−0·010	1334	0·0202	0·0307
−0·005	1064	0·0184	0·0275
0	1013	0·0177	0·0268
0·005	1059	0·0179	0·0274
0·010	1324	0·0200	0·0306
0·015	2637	0·0265	0·0432
0·020	7772	0·0423	0·0742
−0·065	139400	0·2134	0·3143*
0·005	1013	0·0177	0·0268†
0	1247	0·0188	·0297‡

* The *y* coordinate of Ti taken from Kay & Miles (1957).
† The $Pbn2_1$ model.
‡ The *Pbnm* model shown in Table 2.

Table 4. *Interatomic distances* (Å) *and angles* (°) *in* Ti *octahedra*

Standard deviations are in parentheses. The atoms are numbered with lower-case Roman numerals following Sasaki *et al.* (1983).

		$CaTiO_3$	$CdTiO_3$
$\mathrm{Ti^{i}–O(1^{i})}$	× 2	1·9503 (3)	1·9694 (4)
$\mathrm{–O(2^{v})}$	× 2	1·9551 (8)	1·965 (1)
$\mathrm{–O(2^{viii})}$	× 2	1·9587 (8)	1·963 (1)
Mean ⟨Ti–O⟩		1·9547	1·966
Bond-length distortion (×10^3)		0·003	0·002
$\mathrm{O(1^{i})–O(2^{v})}$	× 2	2·778 (1)	2·815 (2)
$\mathrm{–O(2^{iv})}$	× 2	2·776 (1)	2·805 (2)
$\mathrm{–O(2^{i})}$	× 2	2·745 (1)	2·749 (2)
$\mathrm{–O(2^{viii})}$	× 2	2·752 (1)	2·757 (2)
$\mathrm{O(2^{v})–O(2^{viii})}$	× 2	2·754 (1)	2·761 (2)
$\mathrm{–O(2^{iv})}$	× 2	2·781 (1)	2·795 (1)
Mean ⟨O–O⟩		2·764	2·780
$\mathrm{O(1^{i})–Ti^{i}–O(2^{viii})}$		89·51 (5)	89·00 (6)
$\mathrm{O(1^{i})–Ti^{i}–O(2^{v})}$		90·68 (5)	91·36 (6)
$\mathrm{O(2^{v})–Ti^{i}–O(2^{viii})}$		89·43 (3)	89·29 (4)
$\mathrm{O(2^{i})–Ti^{i}–O(2^{viii})}$		90·57 (3)	90·71 (4)

Symmetry code

M(Ca, Cd) (i) $\frac{1}{2} - x, \frac{1}{2} + y, \frac{1}{2} - z$
(ii) $\frac{1}{2} + x, \frac{1}{2} - y, \frac{1}{2} + z$
(iii) x, y, z
(v) $1 + x, y, z$

Ti (i) x, y, z
(ii) $x, y, \frac{1}{2} - z$
(iii) $\frac{1}{2} + x, \frac{1}{2} - y, -z$
(iv) $\frac{1}{2} + x, \frac{1}{2} - y, \frac{1}{2} + z$
(v) $1 - x, 1 - y, -z$
(vi) $1 - x, 1 - y, \frac{1}{2} + z$
(vii) $\frac{1}{2} - x, \frac{1}{2} + y, z$
(viii) $\frac{1}{2} - x, \frac{1}{2} + y, \frac{1}{2} - z$

O(1) (i) x, y, z
(ii) $-x, 1 - y, -z$
(iii) $1 + x, y, z$
(iv) $\frac{1}{2} - x, \frac{1}{2} + y, \frac{1}{2} - z$

O(2) (i) $-1 + x, y, z$
(i′) x, y, z
(ii′) $x, y, \frac{1}{2} - z$
(iii′) $\frac{3}{2} - x, \frac{1}{2} + y, \frac{1}{2} - z$
(iv) $\frac{1}{2} - x, \frac{1}{2} + y, z$
(iv′) $\frac{3}{2} - x, \frac{1}{2} + y, z$
(v) $1 - x, 1 - y, -z$
(vi) $1 - x, 1 - y, \frac{1}{2} + z$
(vii) $-\frac{1}{2} + x, \frac{1}{2} - y, \frac{1}{2} + z$
(viii) $-\frac{1}{2} + x, \frac{1}{2} - y, -z$

Table 5. *Interatomic distances* (Å) *and angles* (°) *with e.s.d.'s in parentheses for cuboctahedron*

		$CaTiO_3$	$CdTiO_3$
$M^{\mathrm{i}}\mathrm{–O(1^{i})}$	× 1	2·359 (1)	2·248 (2)
$\mathrm{–O(1^{iv})}$	× 1	2·473 (1)	2·408 (2)
$\mathrm{–O(1^{iii})}$	× 1	3·051 (1)	3·107 (2)
$\mathrm{–O(1^{v})}$	× 1	3·034 (1)	3·116 (2)
$\mathrm{–O(2^{i'})}$	× 2	2·379 (1)	2·269 (1)
$\mathrm{–O(2^{iv'})}$	× 2	2·617 (1)	2·593 (1)
$\mathrm{–O(2^{v})}$	× 2	2·663 (1)	2·675 (1)
$\mathrm{–O(2^{viii})}$	× 2	3·236 (1)	3·332 (1)
Mean ⟨*M*–O⟩		2·726	2·718
Bond-length distortion (×10^3)		13·37	20·53
$\mathrm{O(1^{i})–O(1^{v})}$	× 2	3·331 (2)	3·197 (2)
$\mathrm{O(1^{v})–O(1^{iii})}$	× 2	4·401 (2)	4·514 (2)
$\mathrm{–O(2^{vii})}$	× 4	2·778 (1)	2·815 (2)
$\mathrm{–O(2^{ii'})}$	× 4	2·776 (1)	2·805 (2)
$\mathrm{O(1^{iv})–O(2^{iii'})}$	× 4	2·745 (1)	2·749 (2)
$\mathrm{–O(2^{vi})}$	× 4	2·752 (1)	2·757 (2)
$\mathrm{O(2^{i'})–O(2^{ii'})}$	× 2	3·253 (1)	3·089 (2)
$\mathrm{O(2^{vii})–O(2^{viii})}$	× 2	4·387 (1)	4·528 (2)
$\mathrm{O(2^{i'})–O(2^{iv'})}$	× 4	2·754 (1)	2·761 (2)
$\mathrm{O(2^{iii'})–O(2^{vi})}$	× 4	2·781 (1)	2·795 (1)
$\mathrm{O(2^{i'})–O(2^{iii'})}$	× 4	4·262 (1)	4·143 (2)
$\mathrm{–O(2^{vii})}$	× 4	4·691 (1)	4·669 (2)
$\mathrm{–O(2^{v})}$	× 2	3·279 (1)	3·148 (2)
$\mathrm{O(2^{iv'})–O(2^{viii})}$	× 2	4·459 (1)	4·578 (2)
Mean ⟨O–O⟩		3·372	3·366
$\mathrm{O(1^{i})}–M^{\mathrm{i}}\mathrm{–O(1^{iv})}$	× 1	87·12 (5)	86·68 (6)
$\mathrm{O(1^{iv})}–M^{\mathrm{i}}\mathrm{–O(1^{iii})}$	× 1	105·13 (4)	109·22 (5)
$\mathrm{O(1^{iii})}–M^{\mathrm{i}}\mathrm{–O(1^{v})}$	× 1	92·63 (4)	93·01 (4)
$\mathrm{O(1^{v})}–M\mathrm{–O(1^{i})}$	× 1	75·12 (4)	71·10 (5)
$\mathrm{O(2^{v})}–M^{\mathrm{i}}\mathrm{–O(2^{vi})}$	× 2	110·93 (3)	115·68 (3)
$\mathrm{O(2^{iii'})}–M^{\mathrm{i}}\mathrm{–O(2^{iv'})}$	× 2	76·86 (3)	73·12 (4)
$\mathrm{O(2^{i'})}–M\mathrm{–O(2^{v})}$	× 2	80·92 (3)	78·63 (4)
$\mathrm{O(2^{iv'})}–M^{\mathrm{i}}\mathrm{–O(2^{viii})}$	× 2	98·72 (3)	100·45 (3)
$\mathrm{O(2^{vii})}–M^{\mathrm{i}}\mathrm{–O(2^{viii})}$	× 2	85·36 (3)	85·62 (3)
$\mathrm{O(2^{i'})}–M^{\mathrm{i}}\mathrm{–O(2^{ii'})}$	× 2	86·25 (3)	85·83 (4)
$\mathrm{O(2^{v})}–M\mathrm{–O(2^{viii})}$	× 2	54·61 (2)	53·37 (3)
$\mathrm{O(2^{viii})}–M^{\mathrm{i}}\mathrm{–O(2^{i'})}$	× 2	56·95 (3)	56·08 (3)
$\mathrm{O(2^{i'})}–M^{\mathrm{i}}\mathrm{–O(2^{iv})}$	× 2	66·70 (3)	68·83 (4)
$\mathrm{O(2^{iv'})}–M^{\mathrm{i}}\mathrm{–O(2^{v})}$	× 2	63·57 (3)	64·07 (3)
$\mathrm{O(1^{i})}–M^{\mathrm{i}}\mathrm{–O(2^{vii})}$	× 2	56·34 (2)	55·17 (3)
$\mathrm{O(1^{v})}–M^{\mathrm{i}}\mathrm{–O(2^{vii})}$	× 2	52·47 (2)	51·64 (2)
$\mathrm{O(1^{v})}–M^{\mathrm{i}}\mathrm{–O(2^{ii'})}$	× 2	60·26 (3)	60·38 (3)
$\mathrm{O(1^{iii})}–M^{\mathrm{i}}\mathrm{–O(2^{ii'})}$	× 2	59·20 (3)	59·08 (3)
$\mathrm{O(1^{iii})}–M^{\mathrm{i}}\mathrm{–O(2^{iii'})}$	× 2	58·04 (3)	58·12 (3)
$\mathrm{O(1^{iv})}–M^{\mathrm{i}}\mathrm{–O(2^{iii'})}$	× 2	65·21 (3)	66·58 (4)
$\mathrm{O(1^{iv})}–M^{\mathrm{i}}\mathrm{–O(2^{vi})}$	× 2	64·68 (2)	65·45 (3)
$\mathrm{O(1^{i})}–M^{\mathrm{i}}\mathrm{–O(2^{vi})}$	× 2	66·85 (2)	69·13 (3)

lographic quantities as interatomic angles and bond-length distortion. All of the $GdFeO_3$-type perovskites define a smooth systematic trend. As t_{obs} decreases, the $O(2^{i})$–$O(2^{viii})$–$O(2^{i})$ [*ab* tilting] angle decreases and $O(2^{i'})$–$O(2^{ii'})$–$O(2^{vii})$ [*bc* tilting] and A–O(1)–B angles increase. Both $CaTiO_3$ and $CdTiO_3$ fit this trend very well using our new data. The older data of Kay & Bailey (1957) for $CaTiO_3$ [$t_{\mathrm{obs}} = 0{\cdot}996$, $O(2^{i})$–$O(2^{viii})$–$O(2^{i}) = 161°$] deviated markedly from the other $GdFeO_3$-type perovskites. Fig. 2 is an example showing the systematic relationships of the tilting of polyhedra in the *ab* plane. Similar relationships are exhibited in the other representations developed by Sasaki *et al.* (1983; Figs. 3–6).

Table 6. *The metal–metal distances* (Å) *and* Ti—O—Ti *and* O(2)–O(2)–O(2) *angles* (°), *with e.s.d.'s in parentheses*

	$CaTiO_3$	$CdTiO_3$
Ti^{i}–Ti^{iii}	3·8262 (2)	3·7927 (2)
–Ti^{ii}	3·8201 (3)	3·8088 (2)
M^{i}–M^{iii}	3·8776 (5)	3·856 (3)
–M^{v}	3·7754 (5)	3·730 (3)
–M^{ii}	3·8408 (3)	3·833 (2)
M^{i}–Ti^{i}	3·3344 (3)	3·3088 (2)
–Ti^{iii}	3·4870 (3)	3·4870 (2)
–Ti^{v}	3·2753 (3)	3·2359 (2)
–Ti^{vii}	3·1664 (3)	3·1437 (2)
Ti^{i}–$O(1^{i})$–Ti^{ii}	156·67 (8)	150·48 (9)
–$O(2^{viii})$–Ti^{iii}	155·71 (5)	149·78 (6)
M^{i}–$O(1^{i})$–Ti^{i}	100·96 (4)	103·15 (5)
M^{iii}–$O(1^{i})$–Ti^{i}	90·63 (4)	91·25 (5)
M^{i}–$O(2^{i'})$–Ti^{v}	97·69 (4)	99·44 (5)
–$O(2^{iv'})$–Ti^{v}	90·25 (3)	89·40 (4)
–$O(2^{iv'})$–Ti^{vii}	86·40 (3)	86·04 (4)
–$O(2^{v})$–Ti^{vii}	85·04 (3)	83·85 (4)
–$O(2^{v})$–Ti^{i}	91·13 (4)	89·63 (4)
–$O(2^{viii})$–Ti^{i}	75·43 (3)	72·16 (3)
–$O(2^{viii})$–Ti^{iii}	80·29 (3)	77·63 (3)
–$O(2^{i'})$–Ti^{iii}	106·60 (4)	110·77 (5)
$O(2^{i})$–$O(2^{viii})$–$O(2^{i})$	150·54 (5)	143·26 (6)
$O(2^{viii})$–$O(2^{i'})$–$O(2^{iv'})$	107·35 (4)	110·98 (5)
$O(2^{i'})$–$O(2^{ii'})$–$O(2^{vii})$	101·77 (4)	104·92 (5)

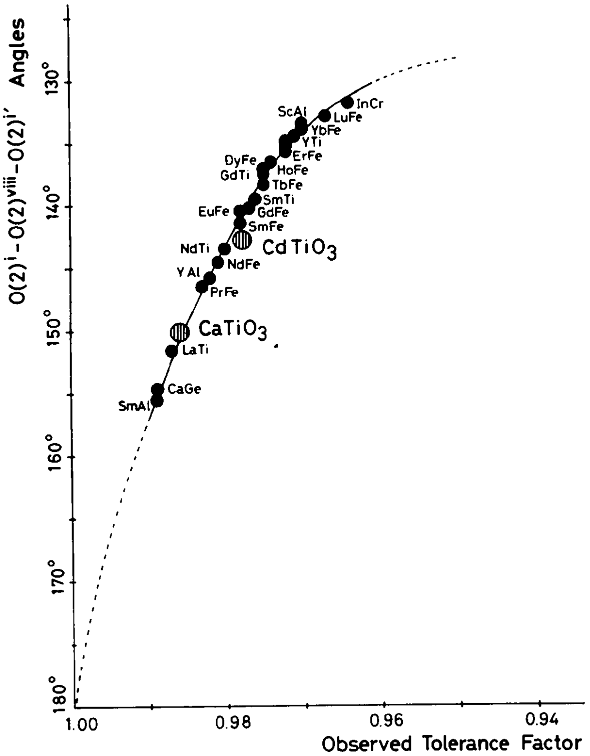

Fig. 2. Tilting of polyhedra near the *ab* plane in terms of $O(2^{i})$–$O(2^{viii})$–$O(2^{i'})$ angles *versus* t_{obs} (after Sasaki *et al.*, 1983).

Results

Analyses of crystal structure and physical properties for $CdTiO_3$ lead us to conclude that there is no reason for $CdTiO_3$ to have a non-centrosymmetric structure with the space group $Pbn2_1$, but rather the space group is *Pbnm* as for most other orthorhombic perovskites. $CaTiO_3$ is also consistent with the *Pbnm* structure. The crystallographic parameters obtained here for these compounds are consistent with the systematic trends found previously among $GdFeO_3$-type perovskites.

The authors thank Professors R. C. Liebermann and R. E. Newnham for various suggestions and discussions. Computations were carried out on the Univac 1110 at the Computer Center of SUNY, Stony Brook. This project has been supported by NSF grants EAR 83-19504 and EAR 82-13513.

References

Becker, P. J. & Coppens, P. (1974). *Acta Cryst.* A**30**, 129–147.

Bish, D. L., Horsey, R. S. & Newnham, R. E. (1979). *Am. Mineral.* **64**, 1052–1055.

Boyd, F. R. & England, J. L. (1960). *J. Geophys. Res.* **65**, 741–748.

Busing, W. R., Martin, K. O. & Levy, H. A. (1963). *ORFLS*. Report ORNL-TM-305. Oak Ridge National Laboratory, Tennessee, USA.

Howells, E. R., Phillips, D. C. & Rogers, D. (1950). *Acta Cryst.* **3**, 210–214.

International Tables for X-ray Crystallography (1974). Vol. IV. Birmingham: Kynoch Press. (Present distributor D. Reidel, Dordrecht, The Netherlands.)

Kay, H. F. & Bailey, P. C. (1957). *Acta Cryst.* **10**, 219–226.

Kay, H. F. & Miles, J. L. (1957). *Acta Cryst.* **10**, 213–218.

Koopmans, H. J. A., van de Velde, G. M. H. & Gellings, P. J. (1983). *Acta Cryst.* C**39**, 1323–1325.

Kurtz, S. K. & Perry, T. T. (1968). *J. Appl. Phys.* **39**, 3798–3813.

Liebermann, R. C., Ringwood, A. E., Mayson, D. J. & Major, A. (1975). *Proc. 4th Int. Conf. on High Pressure, Kyoto*, 1974, edited by J. Osugi, pp. 495–502. Kyoto: Physico-chemical Society of Japan.

Megaw, H. D. (1946). *Proc. Phys. Soc.* **58**, 133–152.

Náray-Szabó, St von (1943). *Naturwissenschaften*, **30**, 202.

Sasaki, S., Prewitt, C. T. & Liebermann, R. C. (1983). *Am. Mineral.* **68**, 1189–1198.

Sholokhovich, M. L., Kramarov, O. P., Proskuryakov, B. F. & Éknadiosyants, E. I. (1969). *Sov. Phys. Crystallogr.* **13**, 967–970.

Tokonami, M. (1965). *Acta Cryst.* **19**, 486.

Wilson, A. J. C. (1949). *Acta Cryst.* **2**, 318–321.

Wuensch, B. J. & Prewitt, C. T. (1965). *Z. Kristallogr.* **122**, 24–59.

Yagi, T., Mao, H. & Bell, P. M. (1978). *Phys. Chem. Miner.* **3**, 97–110.

Acta Cryst. (1987). C**43**, 1674–1675

Thallium(I) Tetrachloroaurate(III)

By Peter G. Jones, Ralf Schelbach and Einhard Schwarzmann

Institut für anorganische Chemie der Universität, Tammannstrasse 4, 3400 *Göttingen, Federal Republic of Germany*

(*Received* 19 *February* 1987; *accepted* 2 *April* 1987)

Abstract. $TlAuCl_4$, $M_r = 543{\cdot}15$, monoclinic, $C2/c$, $a = 12{\cdot}298\,(3)$, $b = 5{\cdot}825\,(2)$, $c = 9{\cdot}681\,(3)$ Å, $\beta = 102{\cdot}09\,(2)°$, $U = 678{\cdot}1\,(7)$ Å^3, $Z = 4$, $D_x = 5{\cdot}32$ Mg m^{-3}, $\mu(\text{Mo}\,K\alpha) = 45{\cdot}6$ mm^{-1}, $F(000) = 912$, $T = 293$ K, $\lambda(\text{Mo}\,K\alpha) = 0{\cdot}71069$ Å, $R = 0{\cdot}067$ for 721 unique observed reflections. The Tl atom lies on the twofold axis 0, y, 0·25 and is coordinated by ten chlorines. The Au atom lies on the symmetry centre 0·25, 0·75, 0·5 and displays the usual square-planar coordination. $TlAuCl_4$ and $RbAuCl_4$ are isostructural.

Introduction. As part of our studies of aurate salts, we have investigated the reaction of thallium(I) hydroxide with tetrachloroauric acid. One product settles out as a dark brown precipitate; this was refluxed with distilled water and the resulting solution (pH 4) left to stand. Small yellow crystals formed.

Table 1. *Atomic coordinates* ($\times 10^4$) *and equivalent isotropic thermal parameters* (Å$^2 \times 10^3$)

	x	y	z	U_{eq}*
Tl	0	2260 (2)	2500	52 (1)
Au	2500	7500	5000	29 (1)
Cl(1)	620 (3)	7336 (7)	4300 (4)	45 (1)
Cl(2)	2694 (4)	4517 (8)	3550 (5)	50 (2)

* Equivalent isotropic U defined as one third of the trace of the orthogonalized U_{ij} tensor.

Table 2. *Bond lengths* (Å) *and angles* (°)

Au–Cl(1)	2·271 (5)	Au–Cl(2)	2·277 (5)
Cl(1)–Au–Cl(2)	90·9 (2)	Cl(1)–Au–Cl(2^{i})	89·1 (2)
Tl···Cl(1)	3·436 (5)	Tl···Cl(2)	3·511 (5)
Tl···Cl(1^{ii})	3·359 (5)	Tl···Cl(1^{iii})	3·350 (5)
Tl···Cl(2^{iv})	3·583 (5)		

Symmetry operators: (i) $0{\cdot}5-x$, $1{\cdot}5-y$, $1-z$; (ii) x, $-1+y$, z; (iii) $-x$, $1-y$, $1-z$; (iv) $-0{\cdot}5+x$, $-0{\cdot}5+y$, z.

Experimental. A needle 0·2 × 0·04 × 0·02 mm was mounted in a glass capillary and used to record 2726 profile-fitted intensities (Clegg, 1981) on a Stoe–Siemens four-circle diffractometer with monochromated Mo $K\alpha$ radiation ($2\theta_{max}$ 60°, quadrants $\pm h{+}k{+}l$ and $\pm h{-}k{-}l$ and some $\pm h{+}k{-}l$ equivalents). Three check reflections showed no significant intensity change. An empirical absorption correction based on azimuthal scans was performed, giving transmission factors 0·18–1·00. Merging equivalents gave 990 unique reflections (R_{int} 0·041); 721 reflections with $F > 4\sigma(F)$ were used for all calculations (program *SHELX*76; Sheldrick, 1976). Index ranges after merging were $|h| \le 16$, $|k| \le 8$, $|l| \le 12$. Cell constants were refined from 2θ values of 47 reflections in the range 19–25°.

The structure was solved by analysis of the Patterson function. Refinement on F (full-matrix) proceeded to R 0·067, wR 0·062 [all atoms anisotropic, weighting scheme $w^{-1} = \sigma^2(F) + 0{\cdot}0004F^2$, 31 parameters, $S = 1{\cdot}74$, max. Δ/σ 0·001, max. and min. features in final $\Delta\rho$ map +2·5 (near Au), −3·5 e Å^{-3}]. The rather high R value is probably associated with residual absorption errors from a strongly absorbing (but relatively weakly diffracting) needle-shaped crystal. Atomic scattering factors used were those of *SHELX*. Final atomic coordinates are listed in Table 1, and bond lengths and

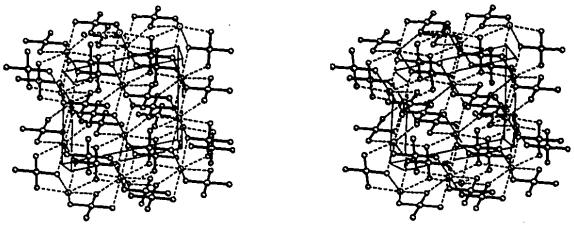

Fig. 1. Stereographic packing plot: view direction slightly rotated from the y axis.

0108-2701/87/091674-02$01.50